ACS OMEGA

http://pubs.acs.org/journal/acsodf

Article

Chitosan Tubes Prefilled with Aligned Fibrin Nanofiber Hydrogel Enhance Facial Nerve Regeneration in Rabbits

Xiaodan Mu,[§] Xiangyu Sun,[§] Shuhui Yang, Shuang Pan, Jingxuan Sun, Yumei Niu,* Lina He,* and Xiumei Wang*

Cite This: *ACS Omega* 2021, 6, 26293−26301

Read Online

ACCESS | Metrics & More | Article Recommendations

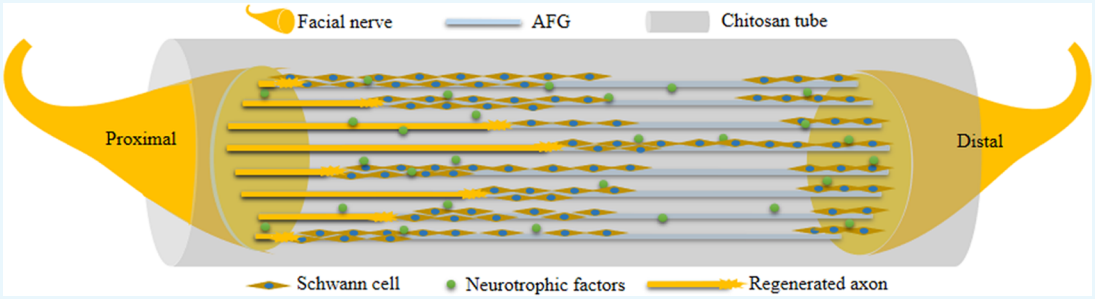

ABSTRACT: Facial nerves are fragile and easily injured, for example, by traffic accidents or operations. Facial nerve injury drastically reduces the quality of life in affected patients, and its treatment presents clinical challenges. A promising therapeutic strategy includes nerve conduits with appropriate fillers capable of guiding nerve regeneration. In this study, a three-dimensional hierarchically aligned fibrin nanofiber hydrogel (AFG) assembled *via* electrospinning and molecular self-assembly was first used to mimic the architecture of the native fibrin cable, which is similar to the nerve extracellular matrix (ECM). AFG as a substrate in chitosan tubes (CST) was used to bridge a 7 mm-long gap in a rabbit buccal branch facial nerve defect model. The results showed that AFG and CST showed good compatibility to support the adhesion, activity, and proliferation of Schwann cells (SCs). Further morphological, histological, and functional analyses demonstrated that the regenerative outcome of AFG-prefilled CST was close to that of autologous nerve grafts and superior to that of CST alone or CSTs prefilled with random fibrin nanofiber hydrogel (RFG), which indicated that AFG-prefilled CST markedly improved axonal regeneration with enhanced remyelination and functional recovery, thus showing great potential for clinical application for facial nerve regeneration treatments.

INTRODUCTION

Facial nerve injury or defects severely impact the quality of life in affected patients, and their treatment remains a significant clinical challenge.[1−3] Axons can regenerate, but fast-growing connective tissue can impede the process of regeneration, and neuroma may occur during slow spontaneous nerve regeneration.[4,5] The most common method for facial nerve transection repair is end-to-end anastomosis by microsurgery, but this method is limited by the length of nerve defects between the proximal and distal end.[6] Autografts are regarded as the gold standard for repairing nerve defects in most clinical cases but suffer from several issues, including lack of host sources, potential cross-infection, requirements of additional surgery, lengthy operation times, as well as mismatches in donor−recipient nerve length/diameter.[7,8] Novel approaches for facial nerve defect repair with similar performance to autografts but fewer associated issues are therefore required.[9] Artificial nerve conduits play an increasingly important role in nerve repair.[10,11] Many strategies have been adopted for the fabrication of effective nerve conduits, such as conditioning with bioactive molecules for release or development of biomimetic platforms.[12−14] However, while conduits are useful for bridging the defects, the functional regeneration is typically extremely limited.[15] Therefore, various studies have strived to find suitable fillings for nerve conduits to improve the functional regeneration following nerve injuries, such as collagen fibers,[16] phosphate-glass fiber bundles,[17] agarose,[18] spongy matrix,[19] and scaffolds.[12] Although conduit fillers have so far mimicked the extracellular matrix for nerve regeneration, a lack of directional neural regeneration was observed. Previous studies have shown that the promotion of directional axonal regrowth is critical for nerve repair.[20−25] Hence, applying

Received: June 29, 2021
Accepted: September 21, 2021
Published: September 30, 2021

directional fillers may be beneficial for improving nerve regeneration.

Fibrin, formed by the reaction of fibrinogen and thrombin, is beneficial for axonal regeneration.[26−31] Considering the hierarchically aligned structure of nerve tissue, it is important to develop a nerve graft that can simulate the anatomical structure of nerve. AFG, an aligned electrospun fibrin bundle, has therefore increasingly attracted attention in the field of nerve regeneration. AFG was first described in a study by Yao et al., where it was shown to promote the neurogenic differentiation of stem cells and the rapid growth of neurites.[30] AFG have not only good biocompatibility and bioactivity, but also function as a biomimetic of the hierarchical structure and mechanical properties of nerve ECM.[30] Since then, AFG has shown promising results for the repair of spinal cord and sciatic nerve injuries,[29,32] but no application in facial nerve repair has been reported yet.

In the current study, we prefilled chitosan tubes (CST), an artificial biodegradable nerve tube widely applied in nerve regeneration research, with AFG for facial nerve defect repair. AFG was generated *via* electrospinning and self-assembly to mimic the native fibrin cable. To explore whether the three-dimensional hierarchical AFG, analogous to the nerve extracellular matrix, could promote axonal regeneration in a rabbit facial nerve buccal branch defect model, AFG and random fiber nanofiber hydrogel (RFG) were initially characterized *via* scanning electron microscopy (SEM), living-cell staining, and CCK8 detection to quantify cell adhesion, activity, and proliferation. These assays demonstrated good biocompatibility of chitosan and fibrin hydrogels with Schwann cells (SCs). CSTs were then prefilled with either RFG and AFG to bridge a 7 mm-long buccal branch facial nerve defect in rabbits. The morphology of the regenerated facial nerve was assessed *via* hematoxylin−eosin (H&E) staining, immunohistochemistry, toluidine blue staining, transmission electron microscopy (TEM), and immunofluorescence staining. Functional recovery was analyzed by vibrissae movement analysis and electrophysiological measurements.

In summary, the aim of this study was to explore the potential of AFG and RFG prefilling of CSTs for facial nerve repair. AFG has potential to provide a novel option for the study and treatment of facial nerve injury repair.

MATERIALS AND METHODS

Preparation of the Chitosan Tube. Sodium hydroxide powder (Boster) was dissolved in distilled water to obtain a saturated solution. After clarification, 56 mL of the above solution were diluted to 100 mL with distilled water. Chitosan powder (6 g) (Yierkang bioengineering company limited, Beijing) was weighed and placed in a beaker, and 2 mL of acetic anhydride liquid and 18 mL of distilled water were subsequently added into the beaker to obtain chitosan solution with a concentration of 30%. It was heated and stirred in a water bath at 50 °C, and 180 mL of distilled water was continuously added to the beaker to finally obtain chitosan solution with a concentration of 3%. A 3% chitosan solution was prepared to coat the lumbar puncture needle (21G, Xiyanghong medical equipment, Guangzhou). The coated lumbar puncture needle was inserted into a 1 mol/L sodium hydroxide solution for 2 min and then rinsed with distilled water. Finally, the chitosan catheter was pulled off the needle and dried thoroughly. The chitosan tubes were cut into 14 mm long and sterilized using cobalt-60 irradiation prior to implantation.

Preparation of Fibrin Hydrogels. Fibrinogen (1 wt %) and polyethylene oxide (PEO, 0.5 wt %) were dissolved in physiological saline to obtain an electrospinning solution, which was then electrospun at a mass flow rate of 3 mL/h under a voltage of 5 kV through a 5 mL syringe with a needle diameter of 0.5 mm. Aligned nanofibers were collected by a rotating collector (50 rpm) containing a $CaCl_2$ (100 mM) and thrombin solution (10 units/mL). Once entering the collector, the fibrinogen immediately formed fibrin after reacting with thrombin. The PEO was then removed from the AFG *via* phosphate-buffered saline (PBS) washes. RFG was obtained by mixing the 1 wt % fibrinogen solution with the thrombin solution (100 units/mL) at the ratio of 10:1. Fibrinogen, thrombin, and PEO were purchased from Sigma-Aldrich.

SEM Observations. After fixation in 2.5% glutaraldehyde for 30 min, the AFG, RFG, and CST samples were dehydrated through an ethanol gradient (30, 50, 60, 70, 80, 90, 95, and 100%) for 20 min each and then dried using a CO_2 critical point dryer (Samdri-PVT-3D, Tousimis). The samples were sputter-coated with a layer of Pt for SEM imaging (JEOL, Japan). In addition, in the SEM experiment of SCs inoculated on chitosan, to facilitate cell inoculation, the chitosan film was made and inoculated with SCs, while SCs were inoculated on the cell slides in the control group for 24 h. The two groups of samples were also fixed after 3 h, and the above steps were repeated.

Cell Activity Assays. Schwann cell lines were purchased from Jiangsu Jingmei Technology Co. Ltd. (Serial number: JDBG190616). SCs were cultured with conventional culture medium (10% fetal bovine serum, 1% penicillin−streptomycin) on the cell slides and chitosan film matched with a 24-well plate at a density of 5×10^4/mL. The samples were collected separately on days 1 and 3, washed twice with PBS, dyed with 200 μL of live-cell dye (Calcein AM, Dojindo), and incubated at 37 °C in the dark for 30 min. Images were acquired using a fluorescence microscope (Olympus, Japan), and the area of living cells was quantified using ImageJ. The cell slides and chitosan film were sterilized using cobalt-60 irradiation prior to implantation.

Cytoskeletal Staining. SCs were cultured on RFG and AFG at a density of 1×10^6/mL. Each treatment was carried out in triplicate (3 wells per group). Samples were collected on the third day, fixed in 4% paraformaldehyde, permeated with 0.1% Triton X100, and blocked with 1% bovine serum albumin (BSA). The samples were then incubated with rhodamine-labeled phalloidin staining solution (1:200, Invitrogen) for 40 min followed by DAPI (Beyotime) staining for 10 min. The samples were then placed under a fluorescence microscope (Leica) for acquisition of images. Statistical analysis was conducted using GraphPad Prism 7.

Cell Proliferation Assay. SCs were cultured on RFG, AFG, or chitosan film at a density of 7×10^4/well. Each treatment was carried out in 5 replicates (five wells per treatment). CCK8 intensities were assessed on days 1, 4, and 7 according to the manufacturer's instructions. Statistical analysis was conducted using GraphPad Prism 7.

Animals and Surgical Procedures. Surgical procedures in rabbits were carried out according to Guides for the Care and Use of Laboratory Animals from the Chinese Ministry of Public Health and U.S. National Institutes of Health. Twenty-four adult New Zealand white rabbits weighing 2.0−2.5 kg,

https://doi.org/10.1021/acsomega.1c03245
ACS Omega 2021, 6, 26293−26301

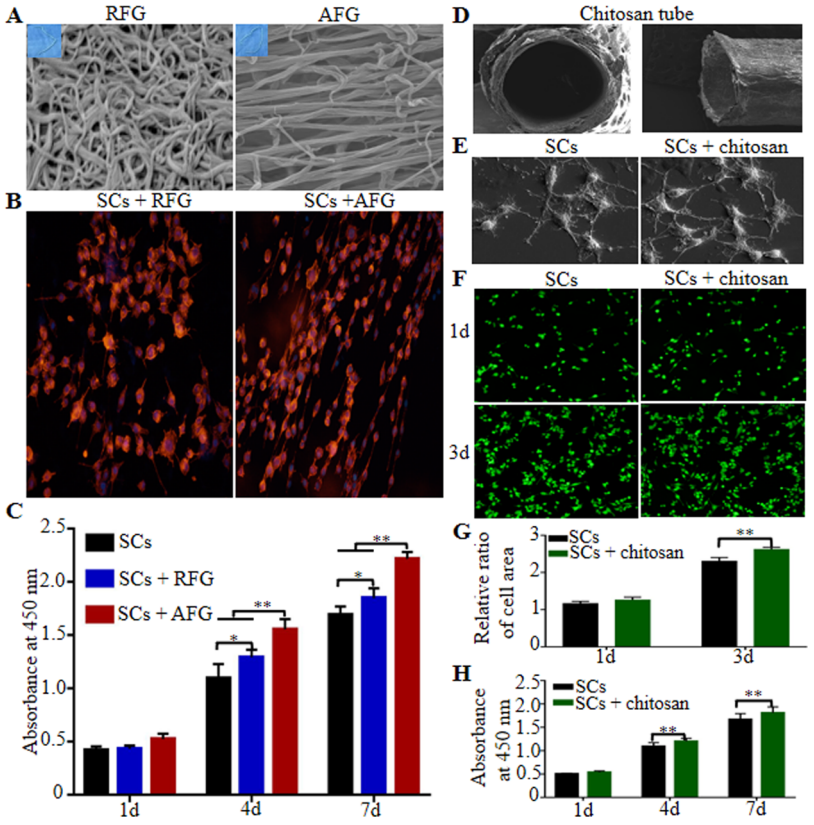

Figure 1. Biocompatibility of fibrin and chitosan with SCs. SEM images of fibrin (A). Directional growth of SCs seeded on fibrin at the 24th hour (B). Proliferation of SCs seeded on fibrin (C). SEM images of the chitosan conduit (D). SEM images of chitosan on the third day (E). Living-cell staining (F) and the statistical results (G) of SCs seeded on the chitosan. Proliferation of SCs seeded on chitosan (H). * $P < 0.05$, ** $P < 0.01$.

provided by Animal Laboratory of Harbin Medical University, were adapted to the natural circadian rhythm and an ad libitum diet for 1 week. Rabbits with normal lip-sipping and beard movements were divided randomly into four groups: empty chitosan tube group (CST group, $n = 6$), chitosan tube prefilled with RFG (RFG group, $n = 6$), chitosan tube prefilled with AFG (AFG group, $n = 6$), and the autograft group (Autograft group, $n = 6$). The animals were anesthetized with pentobarbital sodium (35 mg/kg, iv (intravenous)), and surgery was carried out only once anesthesia was sufficiently deep. The operation area was disinfected and covered with a sterile towel after the cheek hair removal, and the right buccal branch facial nerve of each animal was exposed. A 7 mm segment was excised *via* microsurgery, leaving a gap, which was then bridged with CST, RFG, AFG, or the autografted nerve that was rotated by 180°. Then, the muscle and skin were sutured separately. Rabbits were left to recover for 12 weeks until sacrifice for analysis.

Histomorphological Observation of Regenerated Facial Nerve. *Immunohistochemical Analysis of Regenerated Nerves.* The rabbits were euthanized at 12 weeks after operation *via* anesthetic overdose. The distal segment of regenerative nerve was harvested, followed by postfixing in 4% formaldehyde, embedding in paraffin wax, and transverse sectioning at 3 μm. After blocking with serum, sections were stained with H&E and primary antibodies against neurofilament (NF, Gene Tex) and S100 (Gene Tex). The sections were then incubated with goat anti-rabbit IgG antibodies (Invitrogen) and exposed to hematoxylin to stain the cell nucleus. Finally, images were acquired *via* a fluorescence microscope (Leica) and analyzed using Image-Pro Plus.

Immunofluorescence Staining of Regenerated Nerves. The regenerative facial nerve tissues were sectioned horizontally into 10 μm thick sections 12 weeks after surgery. The paraffin sections were incubated with 0.1% Triton X-100 for 20 min and 1% BSA for 30 min. Then, the sections were stained overnight at 4 °C with NF200 (1:200, Abcam) to visualize regenerated axons and with S100 (1:200, Abcam) to visualize, followed by secondary antibody incubation for 2 h and nuclear counterstaining with DAPI for 10 min. Finally, the horizontal regenerating nerve fibers and SCs were visualized under a fluorescence microscope.

Toluidine Blue Staining and TEM Observation. Twelve weeks after injury, the middle sections of the regenerated facial nerves were fixed in 2.5% glutaraldehyde, postfixed with 1% osmium tetroxide solution, dehydrated in an ethanol gradient series, embedded in the epoxy resin, and then cut into ultrathin 70 nm thick and semithin 700 nm thick sections. The semithin sections were stained with 1% toluidine blue and observed under a light microscope (Olympus Corp) for visualization of regenerated axon density. The ultrathin sections were stained with uranyl acetate and lead citrate and observed using TEM (JEOL, Japan). All images were analyzed using ImageJ.

Functional Evaluation of Regenerated Facial Nerve. *Vibrissae Movement Analysis.* Facial nerve function was examined by three observers every 3 weeks after operation. The whisker function of rabbits was evaluated separately using the following movement scores: 0 indicates no obvious movement, 1 indicates almost imperceptible movement, 2

https://doi.org/10.1021/acsomega.1c03245
ACS Omega 2021, 6, 26293−26301

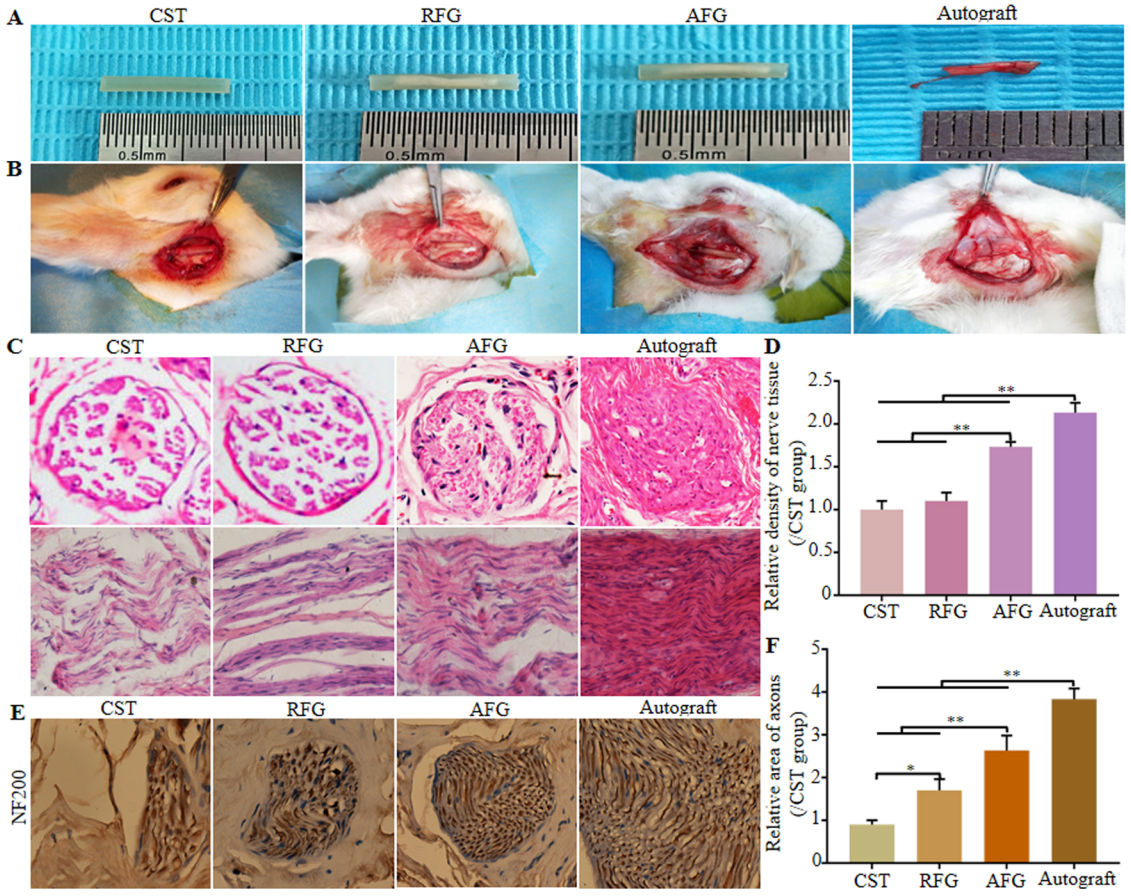

Figure 2. Preparation and implantation of the different groups and histological observation. (A) Gross morphologies of implantation. (B) Graft implantation for bridging the 7 mm rabbit facial nerve defects: CST group: only empty chitosan conduit; RFG group: chitosan conduit filled with RFG; AFG group: chitosan conduit filled with AFG; Autograft group: autograft nerve that was rotated by 180°. (C) Hematoxylin−eosin staining of transverse and longitudinal sections of middle sections from the regenerative nerve at 12 weeks after surgery, and the relative density of transverse sections from the middle segment of regenerated nerve tissue (D). (E) Immunohistochemical staining (NF200, a marker for nerve fiber) of mid-segments from regenerated facial nerve at 12 weeks after surgery and the results of statistical analysis (F).

indicates fewer significant autonomous movement, 3 indicates significant but asymmetric autonomous movement, and 4 indicates symmetric autonomous movement.[31]

Electrophysiological Assessment. Twelve weeks after injury, the buccal branch of the right facial nerve was reexposed under anesthesia for electrophysiological examination (n = 5/group). An electrical stimulation (10 mV) was applied to the buccal branch of facial nerve at a location 5 mm proximal to the graft site and a recording electrode was placed in the buccinator muscle. The stimulation electrode and the recording electrode were used for inducing and recording electrical activity, respectively. The compound muscle action potentials (CMAPs) were recorded using an electrodiagnostic device. Subsequently, the peak amplitude and latency of CMAPs were calculated for statistical analysis (n = 5).

RESULTS

Fibrin Hydrogels and Chitosan Exhibit Good Biocompatibility with SCs. Compared with disordered random fiber nanogel (RFG), AFG was composed of nanofibers, which were aligned along the axis of the fibrin bundle (Figure 1A). SCs cultured on AFG were arranged in parallel to the fibrin bundles, while SCs cultured on RFG were arranged disorderly (Figure 1B). The proliferation of SCs seeded on fibrin hydrogels is shown in Figure 1C. SCs cultured on AFG exhibited higher proliferation than on the other hydrogel groups with the exception of the first day ($P < 0.01$), although the number of SCs cultured on RFG was still higher than on blank culture plates ($P < 0.05$), which demonstrated that fibrin hydrogels generally promote SC proliferation but AFG exhibits an enhanced promotion of proliferation compared with RFG.

The chitosan tube maintained its hollow structure, and SEM did not reveal any collapse (Figure 1D). Chitosan had no effect on the adhesion of SCs (Figure 1E). SC activity is shown in Figure 1F. Chitosan promoted SC activity on the third-day culture (Figure 1G, $P < 0.01$). Moreover, the number of SCs cultured on chitosan was higher than in the control group with the exception of the first day (Figure 1H, $P < 0.01$), which indicated that chitosan also enabled SC proliferation.

AFG Promotes Facial Nerve Regeneration and Remyelination *In Vivo*. Four groups of treatment were assessed for bridging of 7 mm-long gaps in rabbit facial nerves (CST, RFG, AFG, and Autograft). The gross morphologies of grafts and surgical implantations are presented in Figure 2A,B. And when the regenerated facial nerves were harvested in 3 months after operation, no obvious neuroma was found in the operation area.

Transverse and longitudinal middle sections stained by hematoxylin−eosin are shown in Figure 2C. As far as the diameter of regenerated facial nerve is concerned, there was no

https://doi.org/10.1021/acsomega.1c03245
ACS Omega 2021, 6, 26293−26301

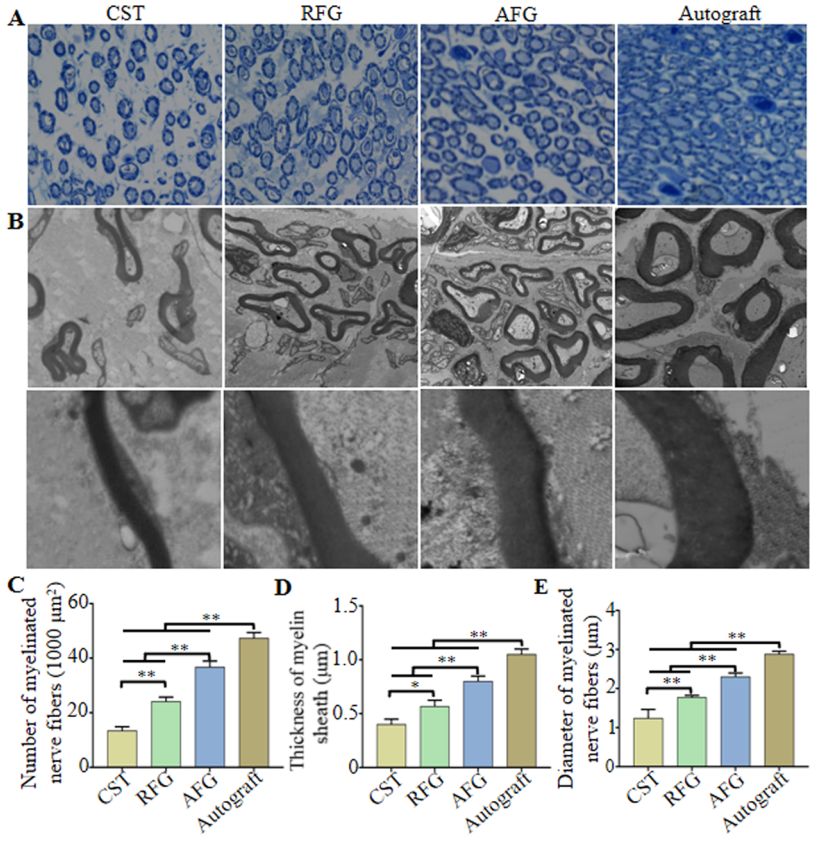

Figure 3. Morphometric analysis of middle sections from regenerated facial nerve 12 weeks after surgery. (A) Toluidine blue staining. (B) TEM images. (C) Number of myelinated nerve fibers/1000 μm^2. (D) Thickness of myelin sheath. (E) Diameters of myelinated nerve fibers. *$P < 0.05$, **$P < 0.01$ ($n = 3$).

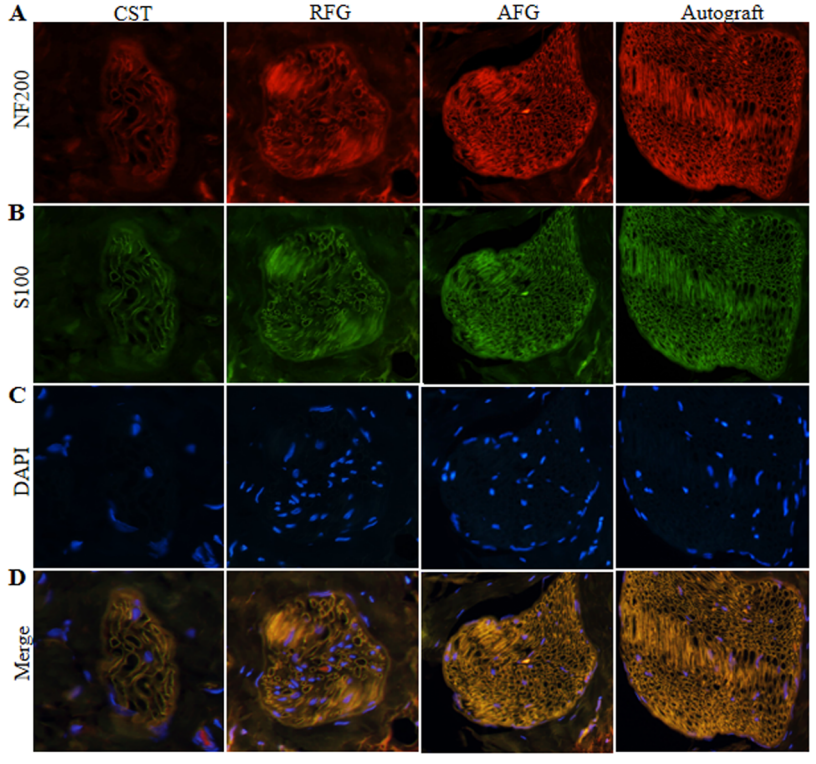

Figure 4. Immunofluorescence staining of mid-sections from regenerated facial nerve 12 weeks after surgery. These sections from four groups were stained with anti-NF200 (a marker for nerve fiber; red) (A), anti-S100 (a marker for myelinating SCs; green) (B), and DAPI (nuclear stain; blue) (C). (D) Merged images of NF200/S100/DAPI labeling.

https://doi.org/10.1021/acsomega.1c03245
ACS Omega 2021, 6, 26293−26301

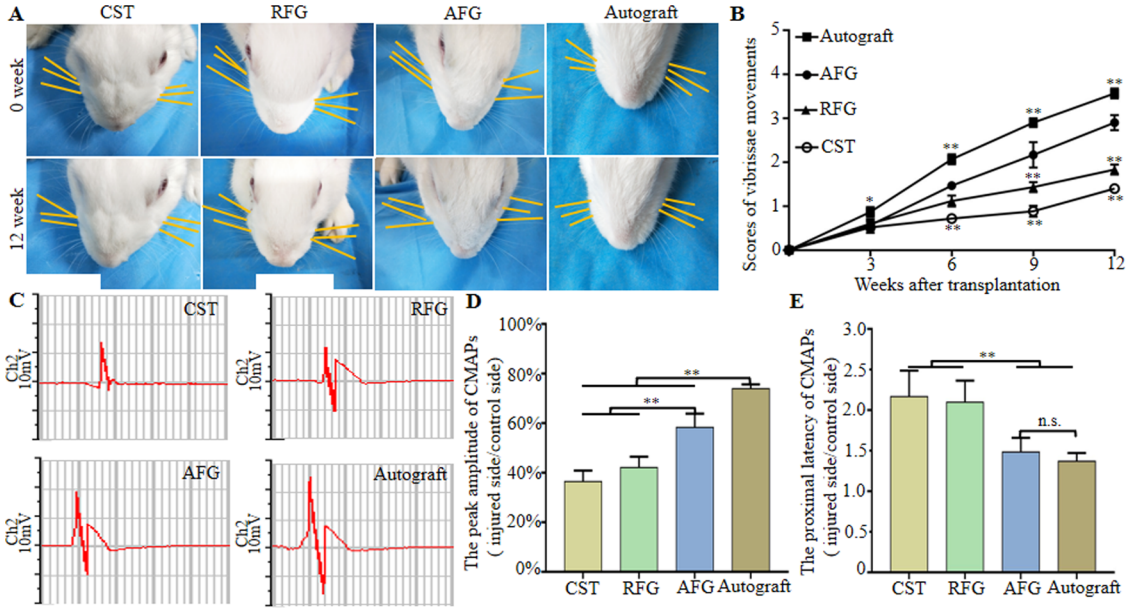

Figure 5. Functional recovery of regenerated facial nerve. (A) Direction of the whiskers (as shown by the yellow line parallel to the corresponding beard for easy observation, and the right side of rabbit was operative side) in four groups at 1 and 12 weeks after surgery. (B) Score of vibrissae movement. (C) Electrophysiological evaluation of regenerated facial nerves 12 weeks after implantation and the statistical results (D) Peak amplitude of CMAPs (injury side/control side). (E) Proximal latency of CMAPs (injury side/control side). *$P < 0.05$, **$P < 0.01$ ($n = 5$).

obvious difference between the groups CST, RFG, AFG, and Autograft. The density of regenerated nerves was higher in the AFG group that in animals treated with CST and RFG, and was closest to the density in the Autograft group, which was consistent with statistical results from transverse sections highlighted in Figure 2D. Transverse distal sections stained by immunohistochemistry of NF200 are shown in Figure 2E. As far as the nerve diameter is concerned, the AFG group was close to the Autograft group compared with groups RFG and CST. The corresponding statistical results showed that the expression of NF200 was significantly higher in the AFG group than in the RFG and CST groups, but as expected lower than in the Autograft group (Figure 2F).

To evaluate the degree of axonal regeneration and remyelination at 12 weeks after surgery, the transverse section of the midportion fibers isolated from the regenerated facial nerve was assessed using toluidine blue staining (Figure 3A) and TEM (Figure 3B). This revealed that there were more myelinated nerve fibers in the AFG and RFG groups compared with the CST group (Figure 3C, $P < 0.01$). Moreover, in both the AFG and RFG groups, the myelin sheath was thicker than in the CST group (Figure 3D, $P < 0.05$) and the diameter of myelinated nerve fibers was likewise higher (Figure 3E, $P < 0.01$). Taken together, this revealed that fibrin nanofiber hydrogels provided a suitable microenvironment for axonal regeneration. Moreover, the myelin sheath thickness and myelinated nerve fiber diameter were greater in the AFG group than in the RFG group (Figure 3C−E), which indicated that AFG exhibited superior qualities for the promotion of axonal regeneration and remyelination than RFG. As expected, the Autograft group showed the most pronounced facial nerve regeneration.

The transverse sections of the middle segments of the regenerated facial nerves were then analyzed by immunofluorescence 12 weeks after the surgery. The sections were stained with NF200 to visualize axons (red) (Figure 4A). Similar to the Autograft group, regenerated axons were abundant and widely distributed in the AFG group. This effect was markedly stronger than in the CST and RFG groups. The sections were then stained with anti-S100 to identify SCs (green) (Figure 4B). The number of S100-positive cells was significantly increased in the AFG group compared to the CST and RFG groups and was similar to the number of S100-positive cells in the Autograft group. Merged images (Figure 4D) revealed that NF200-stained axons were surrounded by profuse S100 staining in the AFG and autograft groups. The above results indicated that AFG promoted axonal regeneration and increased SCs numbers.

AFG Promotes Functional Recovery of the Regenerated Facial Nerve. To assess functional recovery of the facial nerve, vibrissae movement analysis was carried out. One week after the operation, the vibrissae of all rabbits were tilted to the back and whisker movement scores were 0, which indicated a complete loss of function. The vibrissae gradually recovered, but function remained inferior to the uninjured side even after 12 weeks (Figure 5A). Functional recovery, measured every 3 weeks, is shown in Figure 5B, which indicated a gradual score increase of whisker movement in all groups. At weeks 9 and 12, the score in the AFG group was lower ($P < 0.01$) than in the Autograft group but higher than in the RFG and CST groups ($P < 0.01$).

To assess recovery of nerve conduction, an electrophysiological study was performed to record the CMAP. The CMAP amplitude and latency reflect the degree of myelination and the number of innervated muscle fibers, respectively.[32] Figure 5C shows representative CMAP curves 12 weeks after the operation. The peak amplitude in the AFG group was lower than in the Autograft group but significantly higher than in the CST and RFG groups (Figure 5D) ($P < 0.01$). There was no significant difference between amplitudes in the RFG and CST group ($P > 0.05$). The proximal latency in the AFG group was significantly shorter than in the CST and RFG groups ($P < 0.01$) and surprisingly similar to the latency in the Autograft group (Figure 5E) ($P > 0.05$). This electro-

https://doi.org/10.1021/acsomega.1c03245
ACS Omega 2021, 6, 26293−26301

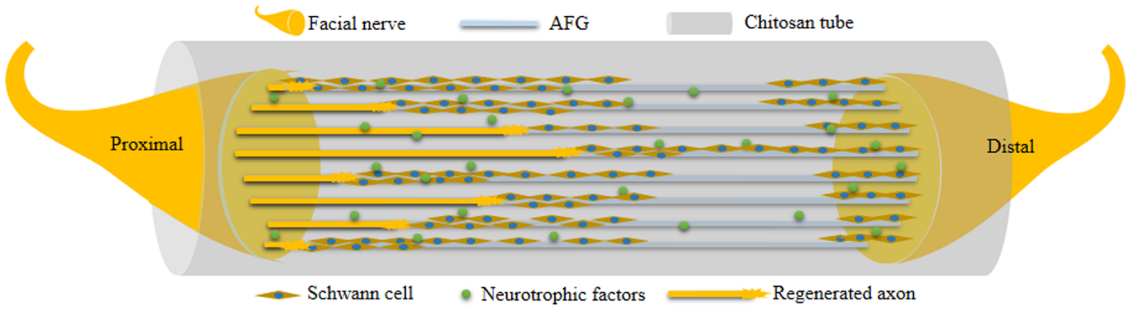

Figure 6. Illustration of AFG bridging and promoting facial nerve regeneration in chitosan tube.

physiological evaluation provided further evidence for functional recovery of regenerated facial nerves repaired with AFG. The above results demonstrated that AFG significantly promoted the recovery of facial nerve conduction.

DISCUSSION

Facial nerve injury significantly reduces the life quality of affected patients and can cause a considerable psychological burden. At present, facial nerve injury repair still faces great clinical challenges. Hierarchically aligned structures are common in nature and have special functions,[33] which may also be important for the physiological repair of nerve tissue.[34] Hence, many nerve grafts are developed based on hierarchically aligned structures to promote nerve regeneration. Here, we prefilled chitosan tubes with AFG, an aligned electrospun fibrin bundle, to bridge facial nerve defects to assess its potential as a clinical treatment strategy.

In *in vitro* experiments, SEM revealed that AFG was composed of fibers that were aligned along the axis of the fibrin bundle, which indicated that the features of AFG imitate natural nerve bundles, indicating that AFG could represent a desirable filler for the construction of a regeneration-promoting microenvironment. When cultured on AFG, SCs adhered directionally along the long axis of aligned fibers and showed better proliferation compared with SCs cultured on RFG, which suggested that AFG has the potential to guide the directional migration of SCs from proximal to distal ends, consistent with previous studies.[32,35] The rapid, directional attachment of SCs, which were considered vital for peripheral nerve regeneration, was considered a prerequisite for axonal regeneration.[22] Chitosan tubes fabricated for this study exhibited good biocompatibility, which is also consistent with a previous study.[36] In fact, to inoculate cells more easily, we made the chitosan membrane matched with the 24-well plate, which indirectly proved the good biocompatibility between SCs and chitosan. Yao et al.[30] inoculated SCs directly on the surface of chitosan tubes, which is more convincing and the current study needs to be improved.

In *in vivo* experiments, the 7 mm defect models of the buccal branch of facial nerve injury in rabbits were successfully established and the defects were repaired separately by nerve grafts in each group. Histomorphological and functional assessments demonstrated that AFG-prefilled chitosan tubes enhanced axonal regeneration and functional recovery compared with CST alone and RFG-prefilled CST. At 12 weeks after the operation, the number and diameter of the myelinated nerve fibers as well as the thickness of the myelin sheaths in the AFG group were similar to the Autograft group. In contrast, few regenerated axons were observed in the CST and RFG groups. H&E, immunohistochemical staining, toluidine blue staining, TEM observation, and immunofluorescence staining confirmed these findings. Indeed, the middle and distal segments of the regenerated facial nerve were sectioned and stained in this study, but the full-length longitudinal sections were not obtained. In Du's study,[32] the longitudinal section of the regenerated sciatic nerve was harvested and stained with NF200, which more directly explained the regeneration effect of sciatic nerve. Moreover, the CMAP amplitudes and latencies of the AFG and Autograft groups were similar. In view of the fact that the CMAP amplitude is positively correlated with the number of nerve fibers and re-innervating target muscles and that the CMAP latency is negatively correlated with myelin thickness,[37] these results indicated that AFG promoted regeneration of fibers across the defect area of the facial nerve and enabled reinnervation of the target muscle. As early as 3 weeks after the operation, the vibrissae movement scores in the AFG group were significantly higher than in the RFG and CST groups, which further verified good functional recovery of the regenerated facial nerve.

In the present study, the beneficial reparative effects were attributed to the CST prefilling with AFG, as shown in Figure 6. The AFG-prefilled CST was used to bridge the proximal and distal end of the nerve. After operation, Schwann cells migrated to the tube from both ends, then arranged along the fibrin bundle and formed directional cell cables. The regenerated axons migrated along this cell cable from the proximal end of the defect to the distal end. The migrated axons were surrounded by Schwann cells to form the myelin sheath. The conduction of the myelinated nerve gradually recovered, and the target organs were innervated again.

AFG, bionic fibrin bundles, may enable facial nerve regeneration because the fiber density is adjustable and the spatial continuity is better than in natural fibrin bundles. Second, the AFG prefilled into CST could waive the construction of natural fibrin cables and accelerate the formation of nerve tissue, shortening the process of facial nerve regeneration. Although regenerated facial nerves may eventually reach their distal target, the earlier nerves reach the target muscles, the earlier the functional recovery of the facial nerve, and the better functional recovery with a lower possibility of irreversible functional injury. In short, AFG may provide a pathway for the migration of SCs during the repair process of the facial nerve. AFG gradually degraded with the invasion of cells and therefore offered more space for axonal migration. In addition, AFG was almost completely degraded 3 months after operation, which matched with the nerve regeneration process and was consistent with the related literature.[18,22] Eventually, regenerated axons participated in the formation of myelin sheaths, working together with SCs, and

https://doi.org/10.1021/acsomega.1c03245
ACS Omega 2021, 6, 26293−26301

achieved a functional recovery comparable to autologous nerve grafts. In addition, the chitosan tube obstructed the invasion of connective tissue and therefore provided enough space for the migration of both SCs and regenerated axons. In summary, our results reveal that CSTs prefilled with the biomimetic AFG may show great potential for the repair of facial nerve defects.

It is worth noting that the degree of facial nerve regeneration observed in the AFG group was not as good as in the Autograft group, which is likely derived from the lack of relevant growth factors such as glial cell-derived neurotrophic factor, nerve growth factor,[38] and brain-derived nerve growth factor.[39] Repair of facial nerve defects is a complicated pathophysiological process,[40,41] and future studies will focus on improving the regeneration of facial nerves using AFG in combination with stem cells and neurotropic growth factors.

CONCLUSIONS

In this study, AFG was applied as a new intraluminal chitosan tube filler to bridge a 7 mm long facial nerve defect in rabbits. *In vitro*, AFG directed SC adhesion and promoted their proliferation. Chitosan displayed good biocompatibility with SCs. *In vivo*, AFG promoted functional recovery of the regenerated facial nerve, with both histological and functional assessments showing improved repair compared to the RFG and CST groups and similar repair compared with the autograft group. In summary, our results reveal that the biomimetic AFG prefilled in chitosan tubes has great potential for the repair of facial nerve defects.

AUTHOR INFORMATION

Corresponding Authors

Yumei Niu − *The First Affiliated Hospital and School of Stomatology, Harbin Medical University, Harbin, Heilongjiang 150001, China;* orcid.org/0000-0002-0312-2498; Email: niuym@hrbmu.edu.cn

Lina He − *The First Affiliated Hospital and School of Stomatology, Harbin Medical University, Harbin, Heilongjiang 150001, China*; Email: helina426@163.com

Xiumei Wang − *Department of Materials Science and Engineering, State Key Laboratory of New Ceramics and Fine Processing, Tsinghua University, Beijing 100084, China;* orcid.org/0000-0002-5303-0217; Email: wxm@mail.tsinghua.edu.cn

Authors

Xiaodan Mu − *The First Affiliated Hospital and School of Stomatology, Harbin Medical University, Harbin, Heilongjiang 150001, China*

Xiangyu Sun − *The First Affiliated Hospital and School of Stomatology, Harbin Medical University, Harbin, Heilongjiang 150001, China*

Shuhui Yang − *Department of Materials Science and Engineering, State Key Laboratory of New Ceramics and Fine Processing, Tsinghua University, Beijing 100084, China*

Shuang Pan − *The First Affiliated Hospital and School of Stomatology, Harbin Medical University, Harbin, Heilongjiang 150001, China*

Jingxuan Sun − *The First Affiliated Hospital and School of Stomatology, Harbin Medical University, Harbin, Heilongjiang 150001, China*

Complete contact information is available at: https://pubs.acs.org/10.1021/acsomega.1c03245

Author Contributions

§X.M. and X.S. contributed equally.

Notes

The authors declare no competing financial interest.

ACKNOWLEDGMENTS

This research was supported by the National Natural Science Foundation of China (no. 81970924), China Postdoctoral Science Foundation Grant (no. 2018M641871), Heilongjiang Province Postdoctoral Science Foundation Grant (no. LBH-Z17177), and Fund of Scientific Research Innovation of The First Affiliated Hospital of Harbin Medical University (no. 2018B018). All of the authors have given final approval and agreed to be responsible for all aspects of the work.

REFERENCES

(1) Ma, F.; Xu, F.; Li, R.; Zheng, Y.; Wang, F.; Wei, N.; Zhong, J.; Tang, Q.; Zhu, T.; Ma, Z.; Xu, F.; Li, R.; Zheng, Y.; Wang, F.; Wei, N.; Zhong, J.; Tang, Q.; Zhu, T.; Wang, Z.; Zhu, J.; et al. Sustained delivery of glial cell-derived neurotrophic factors in collagen conduits for facial nerve regeneration. *Acta Biomater.* **2018**, *69*, 146−155.

(2) Shafaiee, Y.; Shahbazzadegan, B. Facial Nerve Laceration and its Repair. *Traumamonthly* **2016**, *21*, No. e22066.

(3) Spector, J.; Lee, P.; Derby, A. Rabbit facial nerve regeneration in autologous nerve grafts after antecedent injury. *Laryngoscope* **2000**, *10*, 660−667.

(4) Carne, R.; O'Brien, T. J.; Kilpatrick, C.; MacGregor, L. R.; Hicks, R. J.; Murphy, M. A.; Bowden, S. C.; Kaye, A. H.; Cook, M. J. MRI-negative PET-positive temporal lobe epilepsy: a distinct surgically remediable syndrome. *Brain* **2004**, *127*, 2276−2285.

(5) Uz, M.; Sharma, A. D.; Adhikari, P.; Sakaguchi, D. S.; Mallapragada, S. K. Development of multifunctional films for peripheral nerve regeneration. *Acta Biomater.* **2017**, *56*, 141−152.

(6) Greene, J.; McClendon, M.; Stephanopoulos, N.; Álvarez, Z.; Stupp, S.; Richter, C. Electrophysiological Assessment of a Peptide Amphiphile Nanofiber Nerve Graft for Facial Nerve Repair. *J. Tissue Eng. Regener. Med.* **2018**, *12*, 1389−1401.

(7) Ichihara, S.; Inada, Y.; Nakamura, T. Artificial nerve tubes and their application for repair of peripheral nerve injury: an update of current concepts. *Injury* **2008**, *39*, 29−39.

(8) Sun, Y.; Li, W.; Wu, X.; Zhang, N.; Zhang, Y.; Ouyang, S.; Song, X.; Fang, X.; Seeram, R.; Xue, W.; He, L.; Wu, W. Functional self-assembling peptide nanofiber hydrogels designed for nerve degeneration. *ACS Appl. Mater. Interfaces* **2016**, *8*, 2348−2359.

(9) Vasconcelos, B.; Gay-Escoda, C. Facial nerve repair with expanded polytetrafluoroethylene and collagen conduits: an experimental study in the rabbit. *J. Oral Maxillofac. Surg.* **2000**, *58*, 1257−1262.

(10) Gu, X. S.; Ding, F.; Williams, D. F. Neural tissue engineering options for peripheral nerve regeneration. *Biomaterials* **2014**, *35*, 6143−6156.

(11) Faroni, A.; Mobasseri, S. A.; Kingham, P. J.; Reid, A. J. Peripheral nerve regeneration: Experimental strategies and future perspectives. *Adv. Drug Delivery Rev.* **2015**, *82*−*83*, 160−167.

(12) Carvalho, C. R.; Chang, W.; Silva-Correia, J.; Kohn, J. Engineering Silk Fibroin-Based Nerve Conduit with Neurotrophic Factors for Proximal Protection after Peripheral Nerve Injury. *Adv. Healthcare Mater.* **2021**, *10*, No. 2000753.

(13) Barbon, S.; Stocco, E.; Negro, A.; Grandi, C.; Porzionato, A.; Macchi, V.; De Caro, R.; Parnigotto, P. P.; Grandi, C.; et al. In vitro assessment of TAT - Ciliary Neurotrophic Factor therapeutic potential for peripheral nerve regeneration. *Toxicol. Appl. Pharmacol.* **2016**, *309*, 121−128.

(14) Shintani, K.; Uemura, T.; Takamatsu, K.; Yokoi, T.; Onode, E.; Okada, M.; Tabata, Y.; Nakamura, H. Evaluation of dual release of stromal cell-derived factor-1 and basic fibroblast growth factor with

nerve conduit for peripheral nerve regeneration: An experimental study in mice. *Microsurgery* **2020**, *40*, 377−386.
(15) Lu, J. J.; Sun, X.; Yin, H. Y.; Shen, X. Z.; Yang, S. H.; et al. A neurotrophic peptide-functionalized self-assembling peptide nanofiber hydrogel enhances rat sciatic nerve regeneration. *Nano Res.* **2018**, *11*, 4599−4613.
(16) Cao, J. N.; Sun, C. K.; Zhao, H.; Xiao, Z. F.; Chen, B.; Gao, J.; Zheng, T. Z.; Wu, W.; Wu, S.; Wang, J. Y.; et al. The use of laminin modified linear ordered collagen scaffolds loaded with laminin-binding ciliary neurotrophic factor for sciatic nerve regeneration in rats. *Biomaterials* **2011**, *32*, 3939−3948.
(17) Kim, Y. P.; Lee, G. S.; Kim, J. W.; Kim, M. S.; Ahn, H. S.; Lim, J. Y.; Kim, H. W.; Son, Y. J.; Knowles, J. C.; Hyun, J. K. Phosphate glass fibres promote neurite outgrowth and early regeneration in a peripheral nerve injury model. *J. Tissue Eng. Regener. Med.* **2015**, *9*, 236−246.
(18) Carriel, V.; Garrido-Gómez, J.; Hernández-Cortés, P.; Garzón, I.; García-García, S.; Sáez-Moreno, J. A.; del Carmen Sánchez-Quevedo, M.; Campos, A.; Alaminos, M. Combination of fibrin-agarose hydrogels and adipose-derived mesenchymal stem cells for peripheral nerve regeneration. *J. Neural Eng.* **2013**, *10*, No. 026022.
(19) Shuhui, Y.; Chong, W.; Jinjin, Z.; Changfeng, L.; Haitao, L.; Fuyu, C.; Jiaju, L.; Zhe, Z.; Xiaoqing, Y.; He, Z.; Xiaodan, S.; Lingyun, Z.; Jing, L.; Yu, W.; Jiang, P.; Xiumei, W. Self-assembling peptide hydrogels functionalized with LN- and BDNF- mimicking epitopes synergistically enhance peripheral nerve regeneration. *Theranostics* **2020**, *10*, 8227−8249.
(20) Mobasseri, S. A.; Terenghi, G.; Downes, S. Micro-structural geometry of thin films intended for the inner lumen of nerve conduits affects nerve repair. *J. Mater. Sci.: Mater. Med.* **2013**, *24*, 1639−1647.
(21) Mobasseri, S. A.; Terenghi, G.; Downes, S. Schwann cell interactions with polymer films are affected by groove geometry and film hydrophilicity. *Biomed. Mater.* **2014**, *9*, No. 055004.
(22) Yao, L.; deRuiter, G. C.; Wang, H. A.; Knight, M.; Spinner, R. J.; Yaszemski, M. J.; Windebank, A. J.; Pandit, A. Controlling dispersion of axonal regeneration using a multichannel collagen nerve conduit. *Biomaterials* **2010**, *31*, 5789−5797.
(23) Hu, X. J.; Huang, J. H.; Ye, Z. X.; Xia, L.; Li, M.; Lv, B.; Shen, X. F.; Luo, Z. J. A novel scaffold with longitudinally oriented microchannels promotes peripheral nerve regeneration. *Tissue Eng., Part A* **2009**, *15*, 3297−3308.
(24) Gu, Y.; Zhu, J.; Xue, C.; Li, Z.; Ding, F.; Yang, Y.; Gu, X. Chitosan/silkfibroin-based, Schwann cell-derived extracellular matrix-modified scaffolds for bridging rat sciatic nerve gaps. *Biomaterials* **2014**, *35*, 2253−2263.
(25) Kim, Y. T.; Haftel, V. K.; Kumar, S.; Bellamkonda, R. V. The role of aligned polymer fiber-based constructs in the bridging of long peripheral nerve gaps. *Biomaterials* **2008**, *29*, 3117−3127.
(26) Carriel, V.; Garrido-Gómez, J.; Hernández-Cortés, P.; Garzón, I.; García-García, S.; Sáez-Moreno, J. A.; Sánchez-Quevedo, M. C.; Campos, A.; Alaminos, M. Combination of fibrin-agarose hydrogels and adipose-derived mesenchymal stem cells for peripheral nerve regeneration. *J. Neural Eng.* **2013**, *10*, No. 026022.
(27) Wang, Y.; Qi, F.; Zhu, S.; Ye, Z.; Ma, T.; Hu, X.; Huang, J.; Luo, Z. A synthetic oxygen carrier in fibrin matrices promotes sciatic nerve regeneration in rats. *Acta Biomater.* **2013**, *9*, 7248−7263.
(28) Willerth, S. M.; Arendas, K. J.; Gottlieb, D. I.; Sakiyama, S. E. Optimization of fibrin scaffolds for differentiation of murine embryonic stem cells into neural lineage cells. *Biomaterials* **2006**, *27*, 5990−6003.
(29) King, V. R.; Alovskaya, A.; Wei, D. Y.; Brown, R. A.; Priestley, J. V. The use of injectable forms of fibrin and fibronectin to support axonal ingrowth after spinal cord injury. *Biomaterials* **2010**, *31*, 4447−4456.
(30) Yao, S.; Liu, X.; Yu, S.; Wang, X.; Zhang, S.; Wu, Q.; Sun, X.; Mao, H. Co-effects of matrix low elasticity and aligned topography on stem cell neurogenic differentiation and rapid neurite outgrowth. *Nanoscale* **2016**, *8*, 10252−10265.
(31) Farrag, T. Y.; Lehar, M.; Verhaegen, P.; Carson, K. A.; Byrne, P. J. Effect of platelet rich plasma and fibrin sealant on facial nerve regeneration in a rat model. *Laryngoscope* **2007**, *117*, 157−165.
(32) Du, J. R.; Liu, J. H.; Yao, S. L.; Mao, H. Q.; Peng, J.; Sun, X.; Cao, Z.; Yang, Y. C.; Xiao, B.; Wang, Y. G.; et al. Prompt peripheral nerve regeneration induced by a hierarchically aligned fibrin nanofiber hydrogel. *Acta Biomater.* **2017**, *55*, 296−309.
(33) Cui, F. Z.; Ge, J. New observations of the hierarchical structure of human enamel, from nanoscale to microscale. *J. Tissue Eng. Regener. Med.* **2007**, *1*, 185−191.
(34) Rao, F.; Wang, Y.; Zhang, D. Y.; Lu, C. F.; Cao, Z.; Sui, J. J.; Wu, M. J.; Zhang, Y. W.; Pi, W.; Wang, B.; Kou, Y. H.; Wang, X. M.; Zhang, P. X.; Jiang, B. G. Aligned chitosan nanofiber hydrogel grafted with peptides mimicking bioactive brain-derived neurotrophic factor and vascular endothelial growth factor repair long-distance sciatic nerve defects in rats. *Theranostics* **2020**, *10*, 1590−1603.
(35) Li, A.; Hokugo, A.; Yalom, A.; Berns, E. J.; Stephanopoulos, N.; McClendon, M. T.; Segovia, L. A.; Spigelman, I. S.; Stupp, I.; Jarrahy, R. A bioengineered peripheral nerve construct using aligned peptide amphiphile nanofibers. *Biomaterials* **2014**, *35*, 8780−8790.
(36) Boecker, A.; Daeschler, S. C.; Kneser, U.; Harhaus, L. Relevance and recent developments of Chitosan in peripheral nerve surgery. *Front. Cell. Neurosci.* **2019**, *13*, No. 104.
(37) Navarro, X.; Udina, E. Methods and protocols in peripheral nerve regeneration experimental research: part III-electrophysiological evaluation. *Int. Rev. Neurobiol.* **2009**, *87*, 105−126.
(38) Li, R.; Li, D.; Wu, C.; Ye, L.; Wu, Y.; Yuan, Y.; Yang, S.; Xie, L.; Mao, Y.; Jiang, T.; Li, Y.; Wang, J.; Zhang, H.; Li, X.; Xiao, J. Nerve growth factor activates autophagy in Schwann cells to enhance myelin debris clearance and to expedite nerve regeneration. *Theranostics* **2020**, *10*, 1649−1677.
(39) Frostick, S. P.; Yin, Q.; Kemp, G. J. Schwann cells, neurotrophic factors, and peripheral nerve regeneration. *Microsurgery* **1998**, *18*, 397−405.
(40) Johnson, E. O.; Zoubos, A. B.; Soucacos, P. N. Regeneration and repair of peripheral nerves. *Injury* **2005**, *36*, S24−S29.
(41) Colen, K. L.; Choi, M.; Chiu, D. T. Nerve grafts and conduits. *Plast. Reconstr. Surg.* **2009**, *124*, e386−e394.

https://doi.org/10.1021/acsomega.1c03245
ACS Omega 2021, 6, 26293−26301